JOURNAL OF MATERIALS SCIENCE 29 (1994) 4663–4677

Review
The influence of fibre aspect ratio on the deformation of discontinuous fibre-reinforced composites

I. M. ROBINSON*, J. M. ROBINSON
ICI Materials, Wilton Research Centre, P.O. Box 90, Wilton, Middlesbrough, Cleveland TS6 8JE, UK

The fundamental theory for discontinuous fibre reinforcement of plastics is reviewed and compared to experimental data obtained from a range of single-fibre composite tests. Given that the theory provides an adequate description of fibre reinforcement, predictions for the critical fibre length in model composites based on glass fibres embedded in a range of matrices with different volume fractions have been made. The model has been used to predict the modulus for unidirectional discontinuous glass fibre-reinforced composites with a high volume fraction of glass fibres with different mean fibre lengths, diameters and matrices. From this study the concept of a critical aspect ratio, required for effective composite performance, has been defined generally for this type of material. The critical aspect ratio has been found to depend upon fibre diameter, matrix modulus and fibre volume fraction. A brief review of this class of material in the scientific literature has been made in the areas of deformation and failure. To aid the developments in the theory behind discontinuous fibre composites, a series of deformation experiments have been performed on model discontinuous glass fibre/nylon 6,6 compounds produced by extrusion and pultrusion compound technology. The materials were processed using multilive feed technology, to produce effective representations of unidirectional discontinuous glass-fibre composites. Given that the model compounds contained variations in fibre lengths and diameters, the deformation experiments performed were a fundamental test of the theory presented for the critical fibre aspect ratio and the results of theory and experiment have been compared. Based on the predictions of the model and the experimental work, conclusions are offered on the type of fibre that should be used for discontinuous fibre-reinforced composites.

1. Introduction

Discontinuous fibre-reinforced composites form an important category of materials used in engineering applications. Current estimates indicate that 360 000 tonnes of glass fibre-reinforced polymers were produced in 1992 in Western Europe alone [1], with the world consumption of such materials being far larger. Consequently, with such demand from the engineering community for these materials, numerous studies of the mechanical performance of plastic-based engineering compounds exist in the scientific literature. It is well understood that the interface between the polymer matrix and the reinforcing fibre are known to control the mechanical properties in composite materials; however, given that good interfaces can be achieved, choices exist for the type of fibre that can be used in conjunction with a particular polymer matrix. Typical commercial fibres used in discontinuous fibre composites include glass, kevlar and various types of carbon fibres, and the choice is often made on a balance of the engineering properties that can be achieved with a given polymer matrix against the economic cost of manufacture. The type of processing used in these materials is also known to affect the properties from the microstructural level (such as fibre length and orientation), to the mechanical performance of the compound, including stiffness, strength and toughness. With injection-moulding compounds, parts may be made by conventional compounding methods; pultrusion granulated injection moulding represents another alternative. The mean fibre length found in mouldings between these two processing variables can vary from typically 0.2 mm length (for extrusion compounding) to over 1.0 mm (for pultrusion processed material). This variation in mean fibre length with process will affect the eventual mechanical performance.

The aim of this review is to summarize, through the use of a simple, well-established theory, the principles required to produce a good discontinuous fibre com-

* *Present address*: Courtoulds Strategic Research and Technology, P.O. Box 111, Lockhurst Lane, Coventry CV6 5RS.

0022–2461

posite in terms of deformation from both the micromechanical and macromechanical viewpoint. This is described in Section 2 through the concept of a critical aspect ratio (the ratio of the fibre length to diameter) for a particular compound. Reference is made to experimental approaches in the form of single-fibre tests based on a number of techniques such as the application of Raman spectroscopy and fibre-fragmentation tests, which determine at the micro mechanical level the mechanics of the interface. The experimental evidence tends to support the predictions of the simple theory, and on this basis, a model for the stiffness of uniaxial discontinuous fibre-reinforced composites is described in Section 3. The influence of fibre aspect ratio, volume fraction of fibres and the matrix modulus and their role on reinforcement efficiency is described. A review of scientific studies examining the effect of fibre diameter and fibre length on the mechanical performance of such materials is presented. Section 4 presents the results of a creep and recovery study performed on multilive feed glass fibre-reinforced nylon 6,6 compounds, based on both pultrusion and extrusion compounding technology. The materials were chosen as a means of providing a critical test of the predictions of the deformation model. Finally, in Section 5, a set of observations are made on the best choice of fibre geometry for this class of composite material are made, based on the findings in Sections 2 and 3.

2. Micromechanics of deformation for discontinuous fibre composites

In this section the principles of deformation involved in discontinuous fibre composite reinforcement is reviewed based upon the Cox model [2]. The concept of the critical fibre length is discussed and derived from the Cox theory for a general combination of fibre and matrix. Experiments examining the nature of the interface based upon a series of single fibre tests are reviewed and the available data are compared to the mechanics predicted by the Cox model. Finally, the critical aspect ratio has been calculated for a series of hypothetical composites with volume fractions corresponding to single glass-fibre composites ($V_f = 0.001$), and for composites with approximately 30%, 40% and 50% wt/wt glass-fibre reinforcement.

2.1. The Cox model

There have been many models proposed for the micromechanics of fibre reinforcement. These have been reviewed comprehensively by Hollister and Thomas [3], and Chow [4]. Perhaps the simplest model for the micromechanics of discontinuous fibre composite reinforcement is that due to Cox [2], recently reviewed by Asloun *et al.* [5]. The model is described below.

Cox used an analysis known as the classical shear lag theory, which provided a solution to the tensile and shear stress distribution along the length of a fibre embedded in a matrix, provided that certain simplifications are made. These assumptions are:

1. the fibre and matrix remain elastic in their mechanical response;
2. the interface between the two components is perfect,
3. no axial load is transmitted through the fibre ends.

Following these points, the applied stress placed on the matrix parallel to the fibre long axis results in a tensile stress distribution along the fibre length given by

$$\sigma_f = E_f \varepsilon_m \left[1 - \frac{\cosh\beta(\frac{1}{2}l - x)}{\cosh\frac{1}{2}\beta l} \right] \quad (1)$$

This can be rearranged in terms of fibre strain to give

$$\varepsilon_f = \varepsilon_m \left[1 - \frac{\cosh\beta(\frac{1}{2}l - x)}{\cosh\frac{1}{2}\beta l} \right] \quad (2)$$

The shear stress distribution along the fibre length is given by

$$\tau_f = \frac{E_f \varepsilon_m}{2} \left[\frac{E_m}{E_f(1 + \mathrm{vm})\ln(R/r)} \right]^{1/2} \left[\frac{\sinh\beta(\frac{1}{2}l - x)}{\cosh\frac{1}{2}\beta l} \right] \quad (3)$$

where E_f is the fibre modulus, E_m the matrix modulus, l the fibre length, x the position along fibre with length l (x ranges from 0–1), $2R$ the interfibre spacing, $2r$ the fibre diameter, d, vm the matrix poisson ratio and

$$\beta = \frac{2}{d} \left[\frac{E_m}{E_f(1 + \mathrm{vm})\ln(R/r)} \right]^{1/2} \quad (4)$$

Note that for a square fibre packed system, the interfibre spacing can be related to the volume fraction by

$$R = r\left(\frac{\pi}{4V_f}\right)^{1/2} \quad (5)$$

so that β can be rewritten as

$$\beta = \frac{2}{d} \left[\frac{E_m}{E_f(1 + \mathrm{vm})\ln(\pi/4V_f)^{1/2}} \right]^{1/2} \quad (6)$$

The form for the fibre strain, fibre stress and shear stress distributions about a single glass fibre embedded in a nylon 6,6 matrix are shown in Figs 1 and 2. As can be seen from these diagrams the process for load transfer between the matrix and fibre occurs by shear about the fibre ends. About each fibre end the interfacial shear stress is at a maximum, which rapidly decays to zero about the fibre centre. The tensile stress is zero about the fibre ends and rapidly reaches a maximum value about the fibre centre, where the fibre strain matches that applied to the matrix.

From the expressions in the Cox model, a number of points emerge. There are regions about both fibre ends that do not reach the same strain as that applied to the matrix so the reinforcing efficiency is consequently less than that achieved for a continuous fibre composite. The term "critical fibre length" is frequently used to describe the region about both fibre ends where the process of shear stress transfer occurs and the tensile stress in the fibre builds up to reach a maximum value. The exact value for the critical fibre length, l_c, will depend on the definition used. For the purposes of measurement, the critical fibre length has been defined as the length of fibre required to reach 0.9 times the maximum fibre strain, about each fibre end [6] in a long fibre. As pointed out by Galiotis *et al.* [7]

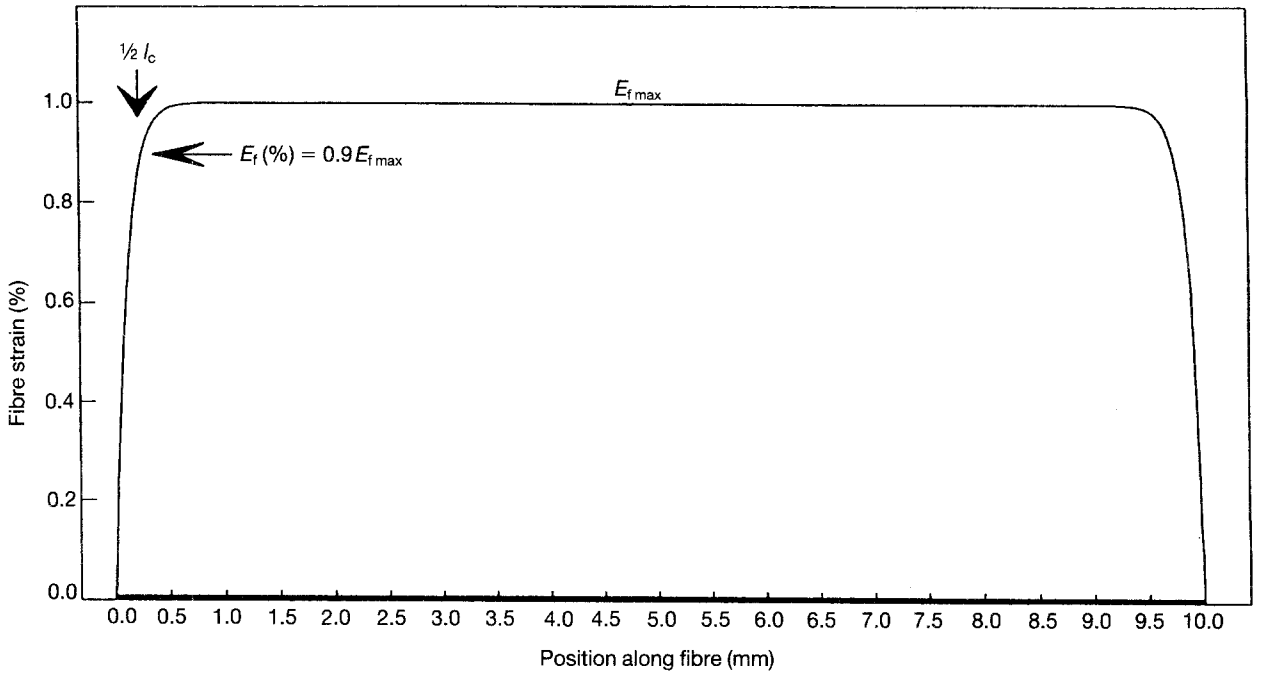

Figure 1 The Cox model prediction for fibre strain distribution. Model for a single glass fibre (d = 17 μm) embedded in nylon 6,6.

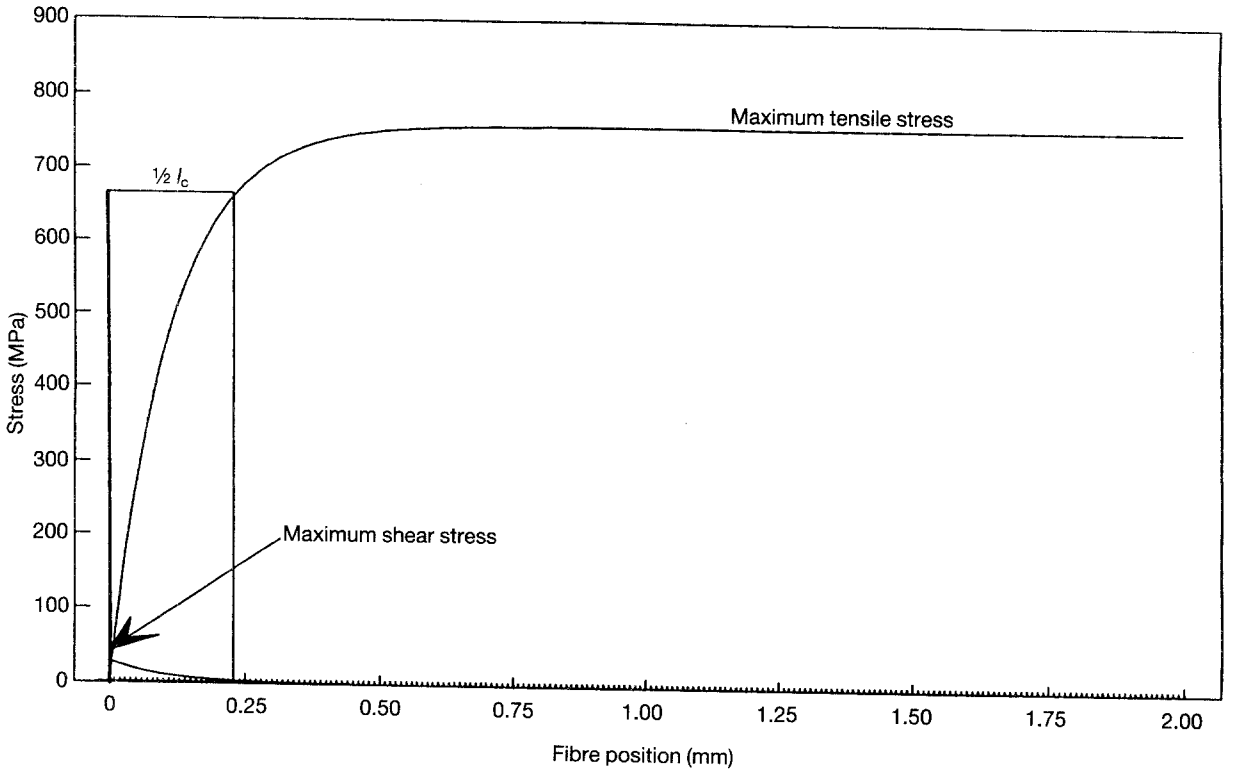

Figure 2 Tensile and shear stress distribution about one fibre end. Model for a single glass fibre (d = 17 μm) embedded in nylon 6,6.

and detailed in other publications [5, 8] the expression shown by Equation 2 can be reduced provided the fibre modulus is greater than the matrix modulus and the fibre length is reasonably long

$$\varepsilon_f = \varepsilon_m\{1 - \exp(-\beta x) - \exp[-\beta(l - x)]\} \quad (7)$$

The ratio of $\varepsilon_f/\varepsilon_m$ reaches the value of 0.9 at certain positions of x along the fibre length. Twice this value of x is taken as the definition of the critical fibre length. Consequently, Equation 5 can be solved for x to obtain the critical fibre length. Thus $\varepsilon_f/\varepsilon_m = 0.9$ at the positions for x when $x = 2.303/\beta$. Direct substitution of these values of x reduces $1 - \exp(-\beta x)$ to the value of 0.9.

Consequently, the critical fibre length, l_c, can be directly determined from the definition of β such that $l_c = 2x$

$$l_c = 2.303d\left[\frac{E_f(1 + \nu_m)}{E_m}\right]^{1/2}\left[\ln\left(\frac{\pi}{4V_f}\right)^{1/2}\right]^{1/2} \quad (8)$$

Under simplification, Equation 8 can be reduced to

$$l_c = Kd\left(\frac{E_f}{E_m}\right)^{1/2}\left[\ln\left(\frac{1}{V_f}\right)^{1/2}\right]^{1/2} \quad (9)$$

The critical fibre length can be seen to depend upon the fibre diameter, the square root of the ratio of the tensile moduli and on a complicated term for the inverse of the fibre volume fraction. The term K represents a constant, involving the collection of all the constant terms in Equation 8 multiplied together.

Similar expressions can be obtained from other analytical models. For the model proposed by Rosen [3, 9] and taking the same definition for the critical fibre length (i.e. $l_c = 2x$, where x gives the result $\varepsilon_f/\varepsilon_m = 0.9$), the critical fibre length can be given by

$$l_c = d\left[\frac{E_f(1 + \nu_m)}{E_m}\right]^{1/2}\left(\frac{1 - V_f^{1/2}}{V_f^{1/2}}\right)^{1/2} \quad (10)$$

Again the critical fibre length can be seen to depend upon the fibre diameter, the square root of the ratio of the tensile moduli and on a complicated term for the fibre volume fraction.

A finite difference analysis solution to this problem by Termonia [10] produced an expression that showed a different dependency on the ratio of the tensile moduli for the fibre and matrix.

$$l_c = Kd\frac{E_f}{E_m} \quad (11)$$

There is clearly a difference in predicted critical fibre lengths as given by the analytical and finite difference analysis solutions contained in Equations 9 and 11, respectively. The next section compares these models against available experimental evidence obtained from single-fibre composite tests in order to resolve this apparent dilemma and to comment on the applicability of shear lag analysis to higher volume fraction composites.

2.2. Experimental measurements of the critical fibre length from single-fibre composites

Given that the interface between fibres and matrices are known to control the mechanical performance of composite materials, a considerable experimental effort has been devoted to studying the micromechanics of the interface. The area has been reviewed recently by Piggott [11, 12], Figueroa *et al.* [13], Narkis *et al.* [14], Galiotis [6], Melanitis and Galiotis [15] and Young [16]. A number of techniques are frequently used, including fibre fragmentation tests, fibre pull-out tests, short beam shear tests, microdebonding and Raman spectroscopy. A brief outline of the findings from two key techniques used in the examination of the interface, those of Raman spectroscopy and fibre fragmentation in the measurement of critical fibre lengths in single-fibre composites are given below.

2.2.1. Raman spectroscopy

Over recent years, a number of Raman active high-modulus fibres have been studied in model single-fibre composites using a technique recently reviewed by Galiotis [6] and by Day and Young [17]. The technique involves the determination of strain via a change in frequency of an active band in the Raman spectra of the fibre. The Raman frequency for a number of high-modulus fibres are known to be linearly dependent upon the fibre strain. Consequently, the Raman band position, hence fibre strain, can be measured point by point along the length of a high-modulus fibre embedded in a resin block under load, thus allowing the strain profile to be determined. Such fibres include polydiacetylene single-crystal fibres and commercially important ones such as Kevlar 49, and a range of carbon fibres. Early studies of single-fibre composites using this technique were based on polydiacetylene–epoxy resin composites [18–21]. Thermal stresses were found to dominate the response of these model systems [18, 19, 21] at low volume fractions, but for samples that were free of residual stresses the fibre strain distribution was found to be broadly in agreement with the findings proposed by the Cox model. The critical fibre length for these composites was found to vary linearly with fibre diameter and was found to increase with applied matrix strain. Both of these observations are predicted from the Cox model as described by Equation 8, with the critical fibre length varying linearly with fibre diameter and with a reduction in matrix modulus due to the linear viscoelastic response of the epoxy with load. It was observed that the strain about the fibre ends remained finite while the composite was under load, in contradiction to one of the assumptions of the Cox model. Nonetheless the strain profiles for the fibres essentially confirmed the predictions of the Cox model.

Model Kevlar 49/epoxy composites have also been examined [6, 22–24] using Raman spectroscopy. Single filaments of Kevlar 49 [6, 22], with diameters in the range 11 μm were introduced into an epoxy to make a uniaxially aligned discontinuous single-fibre composite. The strain profile along the fibre length under a range of applied loads was determined point by point using a Raman microscope. The critical fibre length was determined from this profile and the mean value from six measurements over an applied strain range from 0.5%–1.3% was determined to be 273 μm. Using the quoted values for fibre and matrix modulus, fibre diameter and assuming the volume fraction was approximately 2%, the expression derived for the critical fibre length, Equation 8, gave a predicted critical fibre length of 281 μm. Within the precision of the experiment, the Cox model was seen to give an accurate description of the micromechanics of the model system. Andrews and Young [23] used single filaments of Kevlar 49 and 149 in epoxy and determined the critical fibre length as a function of strain. The fibre strain profiles were qualitatively found to be in agreement with the Cox model and the mean critical fibre length for sized Kevlar 49 fibres was determined to be 253 μm over an applied strain range of 0.4%–1.2%, in good agreement with the data reported by Galiotis [6]. The strain profiles were found to deviate from the Cox prediction at very high strains as the fibre fragmentation process occurred. The effect of varying the size coating on the fibres was also found to influence the critical fibre length for the model system. Andrews *et al.* [24] studied the effect of single-fibre Kevlar 49 fibres, where the fibres were oriented at

angles to the applied stress from 0°–90°. Only the strain at the centre of the fibres was monitored, so the shape of the fibre strain profile with angle was unreported. However, the fibre strain about the centre of the fibre was found to vary with orientation and could be fitted using the expression

$$\varepsilon_f = \varepsilon_o(\cos^2\theta - v\sin^2\theta) \quad (12)$$

Fibres that were oriented about the direction of applied load (i.e. from 0°–30°) were found to reinforce the material, while fibres at larger angles (60°–90°) were found to be subject to compressive strain due to the poisson effect from the epoxy. The critical fibre length in compression was not reported, though this would remain an important parameter to determine to see if it agreed with values measured from the application of tensile load.

Experiments based on carbon fibre/epoxy systems have also been reported [15, 25, 26]. Single filaments of HMS carbon fibre [15] were introduced into an epoxy to make uniaxially aligned fragmentation composites. The test was performed using simultaneously the fragmentation test as proposed by Bascom and Jensen [27] and the Raman spectroscopic technique. During the experiment, the composite was loaded up until fibre fragmentation occurred. After continuously loading the composite, a range of fragmentation lengths was produced which ranged from $l_c/2$ to $4l_c/3$, according to the interpretation of the fibre strengths from an analysis of Weibull statistics. This was recorded from the experiment and the data are reported in Table 2 of [15]. The critical fibre length from the fragmentation test produced a value of 640 μm. The parallel investigation by the Raman technique showed a number of interesting points. The fragmentation test at low strains produced fibre strain profiles similar to that predicted by the Cox model on fibre fragments; at higher strains other effects such as fibre debonding occurred which were strain dependent. These debonded regions lead to a breakdown of the interface, leading to a frictional process of stress transfer. From this a complicated picture of interfacial shear stress transfer was seen to emerge which was strain dependent, with a mean critical fibre length value of 380 μm, as reported in Table I of [15]. The values for the critical fibre length measured by the two techniques can be seen to be different by a factor of approximately two. Given the different nature of the experiments, the Raman spectroscopy approach gave a far more reliable indication of the critical fibre length, particularly before the process of interfacial breakdown occurs. It was also capable of resolving directly the change in mechanism of load transfer. It seems clear from this study that the critical fibre length, as measured from the fragmentation test, essentially involves values determined by a failure process and so does not represent the initial load transfer process. This observation has been confirmed by other studies on single carbon-fibre epoxy resin composites [25, 26]. However, the predictions of the critical fibre length and interfacial shear stress profile based on the Cox model were found to be in reasonable agreement with the experimental data in the limit of low strains. Further applications of this technique to the mechanics of the interface have included an examination of the microdebond test [15]. In general, the experimental Raman data gathered on single high-modulus fibre/epoxy model composites have shown that the Cox model is a reasonable description of the micromechanics of discontinuous fibre composites in the limit of low applied strain, before any failure process begins. The technique is well suited to examine the process of failure, including gross matrix yielding, fibre/matrix debonding and fibre fragmentation, provided the fibres are Raman active and the matrix is reasonably transparent.

2.2.2. Fibre fragmentation tests

The fragmentation test described by Figueroa *et al.* [13], Bascom and Jensen [27] and DiBenedetto [28] has been the most widely adopted method for assessing the micromechanics of composite materials. The studies by Melanitis and co-workers [15, 25], based on a Raman spectroscopic analysis of the test, casts doubt on the precision of the data taken directly from observation; nonetheless, as a method for determining the critical fibre length in discontinuous fibre composites it is still worth reviewing briefly some data from the technique. The test involves incorporating a continuous single filament of fibre into a resin block, then placing the entire system under tensile load. As the load increases, the fibre fragments into discrete lengths when the stress in the filament matches the tensile strength of the fibre at a point along the filament length. The resultant fragmented lengths can be equated to the critical fibre length, with the range of fragmentation lengths varying from $l_c/2$ to $4l_c/3$, according to the interpretation of the fibre strengths from an analysis of Weibull statistics.

Asloun *et al.* [5] collated the results from 14 separate fragmentation tests on a range of thermoset, thermoplastic and elastomeric composites made with a range of fibres. By plotting the ratio of the measured log (critical length/fibre diameter) against the log (fibre/matrix modulus) and performing a regression analysis, a linear fit of the experimental data was found. This was reduced to the expression

$$l_c = k^* d\left(\frac{E_f}{E_m}\right)^{0.44(0.04)} \quad (13)$$

This is similar in form to the expression obtained from the Cox model as expressed by Equation 9. Given that the experiments performed by Melanitis and co-workers [15, 26] has shown that the critical fibre lengths obtained from the fragmentation test are an overestimate, the agreement between the expression suggested by experiment (Equation 13) and the Cox theory (Equation 9) is reasonable, whereas the finite difference analysis proposed by Termonia (Equation 11) [10] gave a poor correlation to the data. Consequently, the Cox model has been seen by two different experimental techniques to give a good description of the mechanics of single fibre composites in the low strain limit, before failure mechanisms come into play.

Asloun *et al.* [5] used a different value of the position x to define the measurement of critical fibre length, so the value of the constant k^* in Equation 12 is different from that given by Equation 8. Nonetheless, the general form fits that given by the experimental data.

2.3. Predicted critical fibre lengths for model composites

Experimental data detailed in Section 2.2 have confirmed that the Cox model gives a reasonable description of the micromechanics of discontinuous fibre composites in the low strain limit. It is of interest to see what the predicted critical fibre lengths for a range of different fibre/matrix composites are, as calculated from Equation 8. The model proposed by Equation 8 assumes that the composites are made from unidirectionally aligned discontinuous fibres, with a square packing arrangement, thought to be the best description for composites with low fibre volume fractions. The fibre was chosen to be E Glass with a modulus of 76 GPa and the matrix to have tensile modulus values at 3.8, 2.8, 1.5 and 0.5 GPa, respectively. The fibre diameters were set at 17 and 10 μm and the volume fraction of fibres at 0.001, 0.16, 0.23 and 0.30. These volume fractions correspond to a single-fibre composite representative of a micromechanical evaluation test (such as the fragmentation test) and to 30% wt/wt, 40% wt/wt and 50% wt/wt glass fibre-reinforced polymer compounds). The data for the predicted critical fibre lengths are shown below in Tables I–IV and the values for the critical aspect ratio (ratio of the critical fibre length to fibre diameter) at the three higher fibre volume fractions are plotted in Fig. 3.

It is clear from these predictions that the critical fibre length values at extremely low volume fractions are much larger than those for composites at higher volume fractions. The critical fibre length shows a marked dependence upon the volume fraction, fibre diameter and matrix modulus. Consequently the data contained in Tables I–IV indicate that for a given fibre and matrix combination, a unique value for the critical fibre length cannot be defined, as the value will change as the matrix displays linear viscoelasticity.

This effect is of relevance when comparing the critical fibre lengths between matrix systems at a common temperature and time, or when considering the critical fibre length for a particular composite at higher temperatures, longer times or high strains, provided that fibre debonding has not occurred. Equation 8 thus accounts for the matrix linear viscoelasticity influencing the critical transfer length, as observed from Raman experiments. The data also suggest that the concept of a critical aspect ratio is of more relevance than a critical fibre length, because fibres will vary in diameter about a mean value due to

TABLE I Predicted critical fibre lengths for a unidirectional discontinuous glass fibre-reinforced composite with $V_f = 0.001$, with varying fibre diameters and matrix moduli

Fibre diameter (μm)	Critical fibre length (μm)			
	$E = 3.8$ GPa	$E = 2.8$ GPa	$E = 1.5$ GPa	$E = 0.5$ GPa
10	222	259	354	613
17	378	441	602	1042
Critical aspect ratio	22.2	25.9	35.4	61.3

TABLE II Predicted critical fibre lengths for a unidirectional discontinuous glass fibre-reinforced composite with $V_f = 0.16$, with varying fibre diameters and matrix moduli. The volume fraction corresponds to 30% wt/wt glass fibre reinforcement

Fibre diameter (μm)	Critical fibre length (μm)			
	$E = 3.8$ GPa	$E = 2.8$ GPa	$E = 1.5$ GPa	$E = 0.5$ GPa
10	109	127	173	300
17	185	216	294	510
Critical aspect ratio	10.9	12.7	17.3	30.0

TABLE III Predicted critical fibre lengths for a unidirectional discontinuous glass fibre-reinforced composite with $V_f = 0.23$, with varying fibre diameters and matrix moduli. The volume fraction corresponds to 40% wt/wt glass fibre reinforcement

Fibre diameter (μm)	Critical fibre length (μm)			
	$E = 3.8$ GPa	$E = 2.8$ GPa	$E = 1.5$ GPa	$E = 0.5$ GPa
10	95	111	152	263
17	162	189	258	447
Critical aspect ratio	9.5	11.1	15.2	26.3

TABLE IV Predicted critical fibre lengths for a unidirectional discontinuous glass fibre-reinforced composite with $V_f = 0.30$, with varying fibre diameters and matrix moduli. The volume fraction corresponds to 50% wt/wt glass fibre reinforcement

Fibre diameter (μm)	Critical fibre length (μm)			
	$E = 3.8$ GPa	$E = 2.8$ GPa	$E = 1.5$ GPa	$E = 0.5$ GPa
10	85	98	135	233
17	144	167	229	396
Critical aspect ratio	8.5	9.8	13.5	23.3

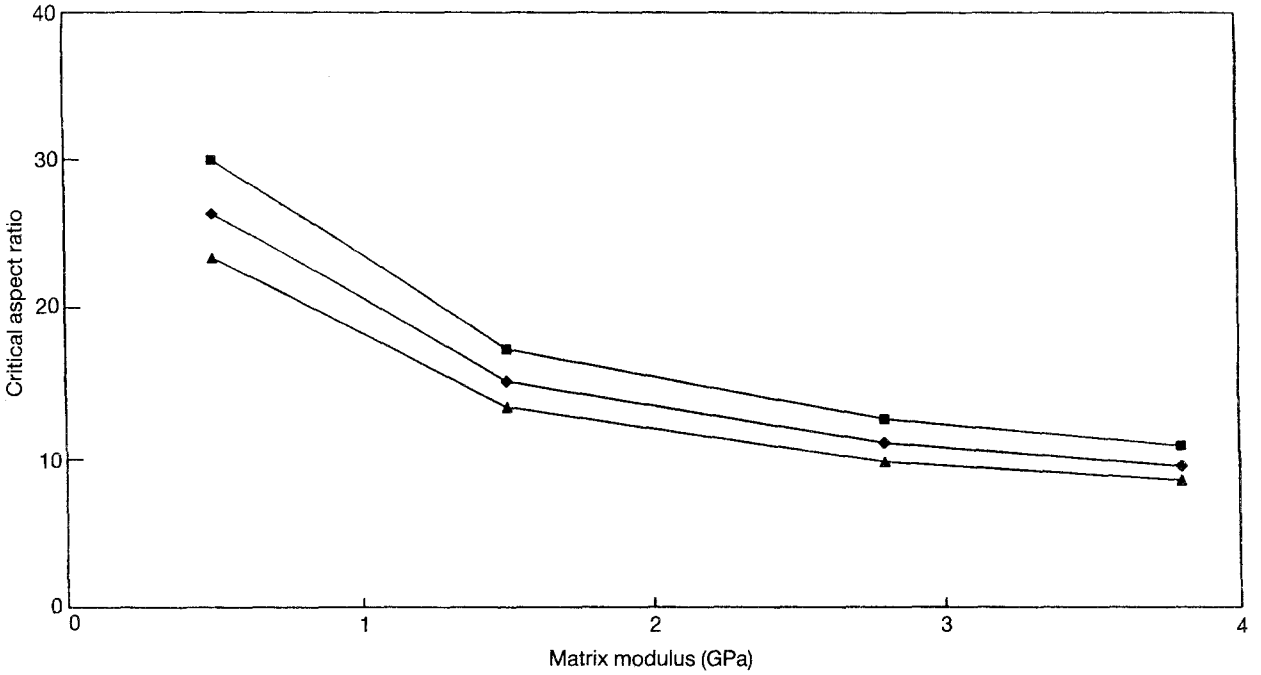

Figure 3 Critical aspect ratio, versus matrix modulus and fibre weight fraction. Data calculated at (■) 30% wt/wt, (◆) 40% wt/wt, and (▲) 50% wt/wt GL/PA 6,6.

production variables, and may be available with the same stiffness at different fibre diameters.

Given the dependence upon all these parameters, the values for critical fibre length obtained in single fibre tests described in Section 2.2, and calculated in Table I, can give a large overestimate for the values found in higher volume fraction composites, as can be seen by comparing values. There is some confidence that the Cox model gives an accurate description of the micromechanics of fibre reinforcement, so at least within the low strain limit the predictions are realistic. The implications for these predicted values of critical fibre length for real composite systems will be discussed further in the next section.

3. Theoretical and experimental studies of discontinuous fibre composites

In this section the effect of mean fibre length and diameter, hence fibre aspect ratio, on the reinforcement efficiency will be studied using a simple model based upon the Cox model. A brief review is also given of studies in the scientific literature that explore the effect of fibre aspect ratio on the mechanical performance of discontinuous fibre composites.

3.1. Theoretical model for the stiffness of discontinuous fibre composites

It can be seen from the Cox model, described in Section 2.1, that a certain length of fibre is required for the transfer of shear stresses from the matrix surrounding embedded fibres in a discontinuous fibre composite under load. The length of fibre over which these shear stresses act is described as being the critical length for the composite and can be calculated from Equation 8. Fibres with lengths less than the critical length do not carry the maximum tensile stress possible from the requirement of having strains match in both phases of the composite (about the centre of the fibre and the matrix), from a simple rule of mixtures approach to the stiffness of composite materials. Fibres with lengths much greater than the critical length act essentially as continuous fibres, in terms of their stiffening contribution. Consequently, the relative efficiency in stiffening the composite can be seen to depend on the fibre lengths found in the composite. A continuous fibre composite, where all the fibre length is available to carry the maximum tensile stress is defined as having 100% reinforcement efficiency. For fibre lengths between very small (fibre length in the order of the fibre diameter) and continuous lie a range

of reinforcing efficiencies between 0 and 100%. Obviously a compromise must be found in maximizing the reinforcing efficiency of the composite for a given combination of fibre, matrix, resultant mean fibre lengths and process technology against the economic considerations in producing such materials.

The critical fibre length will depend upon the fibre/matrix parameters involved according to Equation 8. Using these concepts, it is possible to produce a correction to the stiffness for a unidirectional continuous fibre composite material that takes account of the finite length of fibres in discontinuous fibre composites. The model assumes that the composites are made from unidirectionally aligned discontinuous fibres, with a square packing arrangement. The solution, due to Cox [2] is given below.

A simple rule of mixtures approach to the stiffness of a unidirectional continuous fibre-reinforced composite gives the following equation

$$E_c = E_f V_f + E_m(1 - V_f) \quad (14)$$

For a unidirectional discontinuous fibre-reinforced composite, a correction factor must be introduced to account for the lengths of fibres not fully contributing to the stiffness of the composite, due to the shear stress transfer between each fibre and the matrix. This term, η_l is defined as

$$\eta_l = 1 - [(\tanh \tfrac{1}{2}\beta l)/\tfrac{1}{2}\beta l] \quad (15)$$

The term β is given by Equation 5.

Consequently, the stiffness for the unidirectional discontinuous fibre composite can be expressed by

$$E_c = \eta_l E_f V_f + E_m(1 - V_f) \quad (16)$$

The mathematical limits of this model are worth exploring. For fibre lengths that are very long, the term η_l tends towards unity so the model reduces to that predicted from the rule of mixtures for a continuous fibre composite. For very small fibre lengths (of the order of the fibre diameter) the model should break down because the physical situation becomes that of particulate reinforcement. The value for η_l becomes infinitely large in the limit that the fibre length tends to zero, so it is clear that Equation 15 cannot be applied for composites made from fibres with mean lengths less than five times the fibre diameter and should be replaced by a more appropriate model, describing particulate reinforcement. Within the two limits of fibre lengths described, the model proposed by Cox in Equation 15 has some credibility. It is worth stressing that the analysis assumes the fibre behaves elastically and the matrix behaves with linear viscoelastically, without any breakdown of interfacial bonding due to damage mechanisms that occur at high levels of load. Variables such as strain, temperature and time will effect the reinforcement efficiency for this class of compound. These effects are explored more fully later in this section.

The predicted tensile modulus for a series of unidirectional discontinuous fibre/matrix composites has been calculated using Equation 16. The fibre was chosen to be E Glass embedded in a range of matrices with tensile modulus values at 3.8, 2.8, 1.5 and 0.5 GPa, respectively. The calculations could represent a range of different polymers reinforced with 50% weight fraction glass fibres, under service conditions of low strain and time under load at a constant temperature. Alternatively, the calculations could be taken to represent a particular glass fibre–polymer matrix system, with the polymer matrix modulus varying due to the effect of high strain, increased time under load or variable temperature. The calculations are based on fibre diameters at 17 or 10 μm (typical fibre diameters used in pultrusion- and extrusion-based compounds, respectively) and the volume fraction of fibres was fixed at 0.3, corresponding to 50% weight fraction of glass fibres. The calculations were performed at discrete fibre length intervals of 0.1 mm up to a maximum fibre length of 2 mm. For the purpose of this study, vanishingly small fibre lengths were made to produce the matrix modulus value. The data for these composites, as calculated from Equations 13 and 14 are shown in Figs 4 and 5.

A number of points emerge from these figures. For a given fibre diameter and fibre length the stiffest composite occurs with the highest matrix modulus value. As the fibre length increases, the predicted modulus rises until reaching a plateau value about 2 mm, which is effectively the continuous fibre composite value, with 100% reinforcing efficiency. Comparing the predicted composite modulus for a given fibre length and matrix modulus value across varying fibre diameters also produces comparisons worth noting. At small fibre lengths ($l < 0.5$ mm) the smaller fibre diameter composite produces the stiffest predicted modulus; at identical fibre lengths this is always the case (for example, compare data between Figs 4 and 5 at 0.2 mm length). At increased fibre lengths ($l > 1$ mm), the smaller fibre diameter still produces the stiffest composite, reaching the plateau region earlier than for the larger fibre diameter. This effect becomes particularly pronounced for composites with lower matrix modulus values.

The effects shown in Figs 4 and 5 are a direct consequence of the critical fibre aspect ratio. From the calculation of the tensile modulus for a continuous glass fibre-reinforced composite, it is possible to define

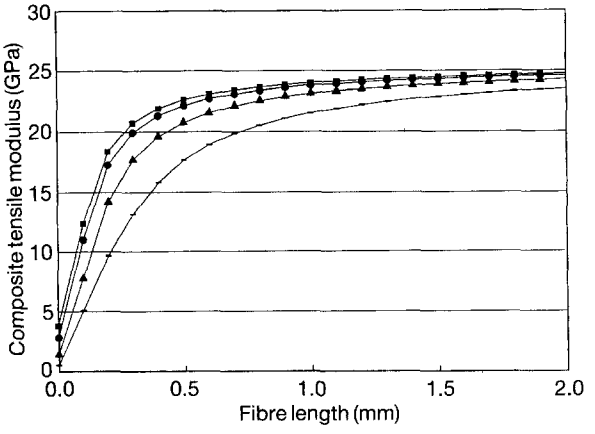

Figure 4 Tensile modulus versus fibre length and matrix modulus. Data calculated for unidirectional 50% wt/wt GL/PA 6,6. E (GPa): (■) 3.8, (●) 2.8, (▲) 1.5, (–) 0.5 GPa. $d = 17$ μm.

a reinforcement efficiency value for η_l such that the discontinuous fibre composite has approximately 90% the stiffness of the continuous fibre composite value, i.e. 90% reinforcement efficiency.

This occurs when the value of η_l equals 0.9, so

$$\eta_l = 1 - \frac{(\tanh \frac{1}{2}\beta l)}{\frac{1}{2}\beta l} = 0.9 \quad (16)$$

This expression can be reduced for large values of the constant β so that

$$\eta_l = 1 - \frac{2}{\beta l} = 0.9 \quad (17)$$

Consequently, η_l will equal 0.9 when

$$l = \frac{20}{\beta} \quad (18)$$

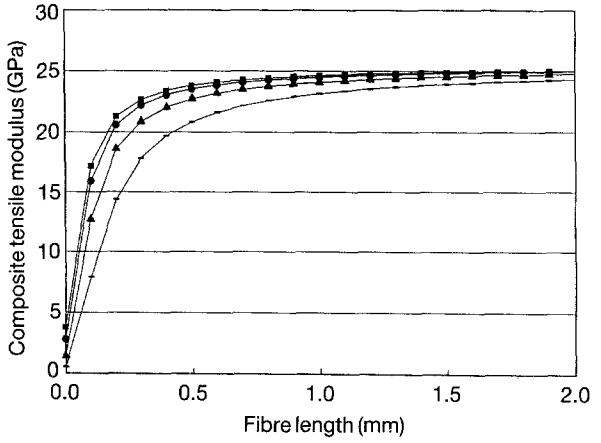

Figure 5 As Fig. 4, for $d = 10\,\mu m$.

From the definition of β given by equation 6 this is achieved for fibre lengths, l, greater than or equal to

$$l = 10d\left[\frac{E_f(1 + \nu_m)}{E_m}\right]^{1/2}\left[\ln\left(\frac{\pi}{4V_f}\right)^{1/2}\right]^{1/2} \quad (19)$$

Comparing this equation to the expression given for the critical fibre length (Equation 8), a reinforcement efficiency of 90% will be obtained for an aligned discontinuous fibre-reinforced composite with fibre lengths approximately four times the critical fibre length or greater. Bearing this in mind, the data contained in Tables II–IV have been recalculated to give the required minimum fibre lengths needed to achieve the stiffness close to that of the continuous fibre-reinforced composite (see Tables V–VII).

The reinforcement efficiency of a discontinuous fibre composite can be seen to depend upon fibre length, diameter and the matrix modulus. With this in mind it is now possible to determine what mean fibre lengths and diameters are required for a high-performing composite material for a given choice of matrix, bearing in mind that the matrix modulus will be varying in service under the influence of variables such as time, temperature, conditioning, etc. Given that in real discontinuous fibre composites the fibre orientation is rarely unidirectional in nature and that orientation is known at the micromechanical level to reduce the achievable stiffness [24], the aspect ratios given in Tables V–VII represent the minimum needed for high-efficiency composites.

The expression given by Equation 19 could also be used to predict the necessary mean fibre lengths for other fibre and matrix combinations. It would also be possible to recalculate the required fibre length and diameter needed to achieve a particular reinforcement efficiency from Equation 17 at a particular volume fraction of fibre.

TABLE V Predicted critical fibre lengths for a unidirectional discontinuous glass fibre-reinforced composite with $V_f = 0.16$, to achieve 90% stiffness of an equivalent continuous glass-fibre composite. The fibre diameters and matrix modulus have been varied. The data for the fibre lengths are based upon the data contained in Table II. The critical aspect ratio (4 × critical fibre length / diameter) is defined at each value for matrix modulus

Fibre diameter (μm)	Critical fibre length (μm)			
	$E = 3.8$ GPa	$E = 2.8$ GPa	$E = 1.5$ GPa	$E = 0.5$ GPa
10	436	508	692	1200
17	741	864	1176	2040
Critical aspect ratio	43.6	50.8	69.2	120

TABLE VI Predicted critical fibre lengths for a unidirectional discontinuous glass fibre-reinforced composite with $V_f = 0.23$, to achieve 90% stiffness of an equivalent continuous glass-fibre composite. The fibre diameters and matrix modulus have been varied. The data for the fibre lengths are based upon the data contained in Table III

Fibre diameter (μm)	Critical fibre length (μm)			
	$E = 3.8$ GPa	$E = 2.8$ GPa	$E = 1.5$ GPa	$E = 0.5$ GPa
10	380	450	610	1050
17	648	756	1032	1788
Critical aspect ratio	38	45	61	105

TABLE VII Predicted critical fibre lengths for a unidirectional discontinuous glass fibre-reinforced composite with $V_f = 0.30$, to achieve 90% stiffness of an equivalent continuous glass-fibre composite. The fibre diameters and matrix modulus have been varied. The data for the fibre lengths are based upon the data contained in Table IV

Fibre diameter (μm)	Critical fibre length (μm)			
	$E = 3.8$ GPa	$E = 2.8$ GPa	$E = 1.5$ GPa	$E = 0.5$ GPa
10	340	400	540	930
17	576	668	916	1584
Critical aspect ratio	34	40	54	93

3.2. Experimental studies of the effect of fibre geometry on the deformation and toughness of discontinuous fibre composites

In order to explore the influence that the mean fibre length, diameter and the matrix modulus has on the mechanical performance of discontinuous fibre-reinforced composites, a brief review of the scientific literature has been conducted, limited to papers studying these effects.

The effect of fibre length was predicted for this type of material by Laws and McLaughlin [29] who found, using a self-consistent analysis, that fibres with aspect ratios of about 100 acted essentially as continuous fibres in a composite. This study assumed constant values for fibre diameter.

Experimental studies have been reported on materials made by long-fibre impregnation technology, including studies by Gore *et al.* [30], Davies *et al.* [31], Moore *et al.* [32] and Bailey *et al.* [33, 34]. It is generally understood that long-fibre-reinforced composites produce stiffer, stronger and tougher materials than equivalent short-fibre materials. Some studies have tried to compare the mechanical performance directly for equivalent compounds based on short- and long-fibre technology. The results from these studies are given below.

Moore *et al.* [32] took equivalent weight fractions (40% wt/wt) of short and long glass fibre-reinforced polypropylene and examined them using a range of experimental techniques based on creep, creep rupture and fatigue. The composites based on short-fibre technology had a mean fibre diameter and aspect ratio of 11 μm and 32, respectively; the long-fibre composites had a mean diameter and aspect ratio of 17 μm and 82, respectively. The mouldings were found to be complex in terms of their microstructure and the short-fibre compound was found to have a higher volume fraction. Short-term stiffness measurements showed no real difference between the two compounds. However, once the influence of time and temperature came into effect through a creep experiment at elevated temperature, the long-fibre composite outperformed the short-fibre compound (see, for example, Figs 5 and 6). This can be explained by the values for the mean aspect ratio of the two compounds. Comparing the values given above with the values quoted in Table VI for a matrix with a modulus of between 1.5 and 0.5 GPa, it is clear that the long-fibre compound had a greater percentage of fibres which exceed the mean aspect ratio suggested for improved performance, compared to the short-fibre compound. These results are in accord with the basic principles outlined in Section 3.1.

An examination of the toughness for long and short glass fibre-reinforced polyamide by Carling and Williams [35] produced an interesting set of data. The composites based on short-fibre technology had a mean fibre diameter and aspect ratio of 13 μm and 19, respectively; the long-fibre composites had a mean diameter and aspect ratio of 17 μm and 26, respectively. It was thought that the mean fibre lengths in the long-fibre compound (450 μm) were small compared to typical compounds prepared by this technology and so represented the material under the worst processing conditions. The fracture strength and toughness was examined for these compounds in the dry and 50% conditioned state, using a notched three-point bend geometry, by Izod pendulum impact and by a slow crack growth approach. Little difference was found for the toughness of the two materials under the dry state under either impact or slow crack growth conditions, however, under 50% humidity the long-fibre compound was found to be tougher by both techniques. Given the inherent complications of studying toughness in such materials, the authors attempted to explain their observed results on the basis of the difference of fibre geometry used in such materials. Developing this theme further with the predictions described in Section 3.1, it is clear there is a small improvement in the mean aspect ratio for the long-fibre compounds tested compared to the short-fibre compound. The values compare to the predicted value of critical aspect ratio of 40, obtained from Table VII for a matrix material with a modulus of 2.8 GPa. The differences in critical aspect ratio are not great, so little difference in performance might be expected. Under increased matrix humidity the matrix modulus will tend towards lower values, thus increasing the required value of critical aspect ratio needed for effective reinforcement, assuming that the interface remains perfect under these conditions. Consequently, it would be expected that the long-fibre compound would benefit under these more extreme conditions. This was observed in the study.

The effect of fibre diameter has been studied by a number of authors, including Ramsteiner and Theysohn [36–38] and Sato *et al.* [39]. Ramsteiner and Theysohn [36–38] studied the mechanical performance of short fibre-reinforced polyamide at two separate weight fractions with fibres ranging in diameter from 10–24 μm. It was found that greater fibre

lengths were retained for compounds made from smaller fibre diameters, but the mean aspect ratios were approximately constant at about a value of 20 for compounds made from 40% wt/wt glass fibre. The mechanical properties measured were the tensile modulus, strength and notched Charpy impact strength under dry conditions and at a range of temperatures. The tensile moduli determined across a range of weight fractions showed an improvement in modulus with decreasing fibre diameter for the compounds at higher volume fraction. This pattern of property enhancement with decreasing fibre diameter was also observed in the tensile strength measurements made across a range of temperatures, and for the notched Charpy impact strengths at all temperatures. Overall the best mechanical performance was measured on the compound made from the smallest fibre diameter at 10 μm. This result is in accordance with the expectations from the model described in Section 3.1, given the mean aspect ratios obtained from the compounds.

Akay and Barkley [39] studied a series of long- and short-fibre 50% wt/wt glass fibre nylon 6,6 compounds in a rectangular mould in an attempt to understand the relationship between fibre orientation and mechanical behaviour as a function of position in the mould and under different moulding conditions. Multilayered fibre orientations were found in each test specimen and were strongly influenced by the position of the specimen in the mould and by the moulding conditions. A strong correlation was found between ultimate tensile strength and tensile stiffness with the size of the core region; in general, test specimens with larger cores were found to have reduced properties. Equivalent points in the mould were compared between long- and short-fibre compounds and in all measured areas of mechanical performance (including modulus, strength and LEFM toughness) the long-fibre compound was found to have equivalent or superior properties compared to the short-fibre compound.

Sato *et al.* [40] studied the mechanical performance of short fibre-reinforced polyamide at 30% weight fractions with fibres ranging in diameter from 0.5–13 μm. It was found that greater fibre lengths were retained for compounds made from smaller fibre diameters up to a limit of 7 μm, with increased mean aspect ratios for smaller fibre diameters. The values quoted for the mean aspect ratio for compounds made from 7 μm fibres was 60; the compound at 13 μm had a mean aspect ratio of 20. The fibre-length distributions, however, looked similar for the compounds at these two fibre diameters. The mechanical properties measured were the tensile and flexural modulus, strength and both notched/unnotched Charpy impact strength under dry conditions and at 23 °C. The tensile and flexural moduli determined across the range of fibre diameters showed a peak performance level for the compounds made with 7 μm diameter fibres, with a severe loss of stiffness for the compounds made from 0.5 μm diameter fibres. This pattern of property enhancement with decreasing fibre diameter was also observed in the tensile strength measurements and for the notched Charpy impact strengths at all temperatures, with the exception of compounds made from small fibre diameters. The reduction of properties at extremely low fibre diameters was accounted for by a micromechanical failure model described in more detail below.

Sato *et al.* [40, 41] also studied the micromechanics of discontinuous fibre-reinforced composite failure by examining glass fibre reinforced polyamide 6,6 under three-point flexure in an SEM. The process they described is shown graphically in Fig. 15 from Sato *et al.* [40]. The first failures in the composite initiated at the fibre ends by a process of debonding. These microcracks propagated along the fibre interface, also causing voiding about the fibre ends. Gradually as the load increased, the matrix material began to shear yield. These bands tended to run between fibre ends, where the shear stresses were concentrated. Eventually the applied strain increased to such a level that slow cracks grew in the yield bands, finally becoming a fast crack. This rapidly spread through the material, and a large amount of fibre pull-out was seen to occur. Little direct evidence of fibre failure was seen until the final stage of composite failure. In an earlier study, Sato *et al.* [40] analysed by direct observations with an SEM the failure process for composites based on glass fibres with different fibre diameters embedded in polyamide 6,6. They noted that the higher observed strength and toughness values found for smaller fibre diameters could be explained by the following process.

Failure at the interface was seen to occur first, so consequently a good interfacial bond was a prerequisite for a good composite. For a composite made with a constant weight fraction of fibres but smaller fibre diameter, more fibres are necessarily present, thus increasing the total amount of interface in the material for stress transfer (this, of course, is the principle mechanism for achieving a stiffer composite with the same mean fibre length but smaller fibre diameter as described earlier in this paper). Secondly, more fibres are present in small fibre diameter composites, leading to a reduced average interfibre separation. This acts to increase the interfibre interaction, reducing the fibre stress concentration about the fibre ends, thus suppressing the onset of debonding/shear yielding. With an increased total number of fibres, the eventual crack path length during the final stages of failure must be greater for a composite with smaller fibre diameters but the same mean length, because more fibres are present. Longer fibres will, of course, increase this toughening mechanism further with the ideal case being achieved for long fibres with small fibre diameters. Finally, a larger total number of fibre ends increases with decreasing fibre diameter which suggests that more sites for damage will occur in the limit of very small fibre diameter fibres ($d < 4$ μm). This would act as the effective limit on the strength-enhancing mechanism for small fibre diameters, as outlined above.

Overall, a number of studies have suggested experimental data in terms of stiffness that match the general trends explained in the model for discontinuous fibre composites, with strength and toughness values also

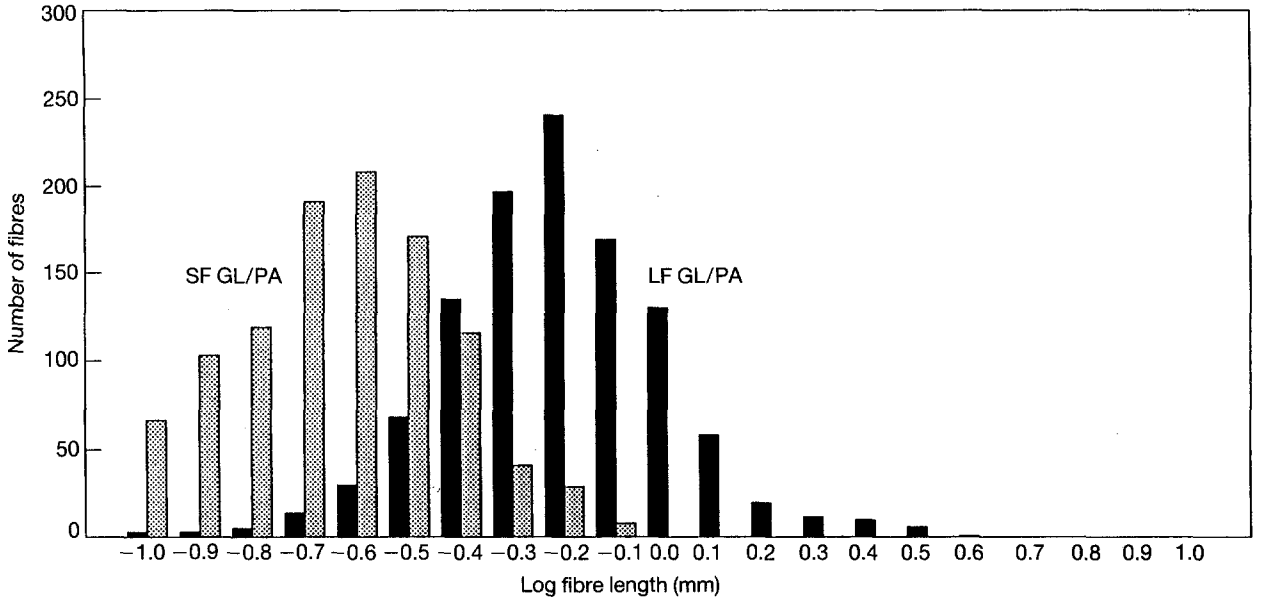

Figure 6 Fibre length distributions for LF GL/PA and SF GL/PA. Multilive feed processed 50% wt/wt glass fibres.

following the same trend. A general improvement in mechanical property performance has been seen for composites with longer fibre lengths or from the use of smaller fibre diameters. These enhancing effects might be in conflict with each other in terms of processing science for the case of long-fibre technology, but for the case of short-fibre technology it is clear that improvements in performance seem possible for compounds based on smaller fibre diameters. The key parameter with each type of technology would imply the requirement of large fibre aspect ratios in the final moulded components.

4. Experimental study of the effect of fibre aspect ratio on stiffness in discontinuous fibre composites

In order to test further the understanding developed above and to remove as much as possible the skin/core/skin microstructural effects noted in the literature [32, 40], a series of 50% wt/wt glass fibre-reinforced nylon 6,6 materials based on extrusion and pultrusion compounding have been produced using multilive feed technology. Because it is well understood that multilive feed mouldings have a greatly improved fibre orientation compared to mouldings produced by standard injection moulding, the materials under test are a good approximation to an injection-moulded unidirectional discontinuous fibre composite. In Section 4.1 the materials are described in more detail. In Section 4.2, the creep deformation for these materials is reported and the results are interpreted in terms of the critical aspect ratio for the two compounds.

4.1. Materials

The two injection moulding materials were based on 50% wt/wt (30% by volume) glass fibre-reinforced nylon 6,6. The short-fibre-reinforced compound was prepared by commercial extrusion compounding using fibres with a mean diameter of 10 μm. The long-fibre material was made using pultrusion technology using fibres with a mean diameter of 17 μm. The length of the granules used for the pultrusion compound was 10 mm, which equalled the length of the continuous glass fibre in the compound. The compounds were processed using multilive feed technology in a mould with dimensions 180 mm × 60 mm × 3 mm; samples oriented parallel to the direction of mould flow were machined from the resultant plaques. The fibre length distribution and orientation distributions were determined from the centre of each moulding. The orientation of the fibres was found to be similar between each type of material; little evidence was found of a core region about the centre of the mouldings, which is in contrast to materials prepared by standard injection moulding.

TABLE VIII Mean fibre lengths and volume fractions determined for the long and short glass fibre nylon multilive feed compounds

Material	Mean fibre length, $\langle l \rangle$ (mm)	V_f (%)
Long-fibre GL/PA	0.58	29.5
Short-fibre GL/PA	0.21	28.3

The fibre length distributions for the two materials were determined using an image analysis approach described more fully elsewhere [33]. The mean fibre lengths are quoted above in Table VIII, together with the fibre volume fractions. The fibre length distributions for the materials are given in Fig. 6. From these data it is clear that the long-fibre GL/PA compound has a mean length approximately 2.5 times longer than the short-fibre GL/PA compound, despite the fibre lengths for both compounds undergoing attrition from the multilive feed process.

4.2. Creep study on long and short glass fibre-reinforced nylon multilive feed compounds

Tensile creep measurements were performed on both long and short GL/PA specimens machined from the test panels using the methods described by Turner [42]. The specimens were dried prior to testing to remove any influence of moisture on the materials. 100 s isochronous tensile stress–strain curves were determined at 23 and 120 °C; subsequently creep tests were performed at the same temperatures up to 10^5 s.

The creep modulus data for the two compounds at 23 and 120 °C are shown in Fig. 7. The data have been interpolated to show the creep modulus of both compounds at a common strain of 0.2% at 23 °C and at 120 °C. From Fig. 7, it is clear that the long-fibre compound has a higher modulus compared to the short-fibre compound at both 23 and 120 °C, at all times under load. However, it is interesting to note that the relative difference between the stiffness of the two compounds increases with temperature.

This may be explained by reference to the data shown in Tables IV and VIII. The mean fibre lengths for the compounds given in Table VIII can be compared to the critical fibre lengths given in Table IV. The critical fibre lengths have been taken from Table IV at a matrix modulus values of 2.8 GPa (corresponding to the low strain time under load modulus for nylon at 23 °C) and at 0.5 GPa (corresponding to the low strain time under load modulus for nylon at 120 °C).

Also given in Table (IX) are the percentages of fibres (as determined from Fig. 6) that exceed the critical fibre length for these compounds at the two temperatures under consideration. At 23 °C, the majority of fibres in both the long- and short-fibre compounds exceed the critical fibre lengths relevant to their fibre diameters, as determined from Table IV. The increased fibre length distribution for the long- fibre compound results in the higher creep modulus compared to the short-fibre compound, following the mechanics described in Section 3.1. At the elevated

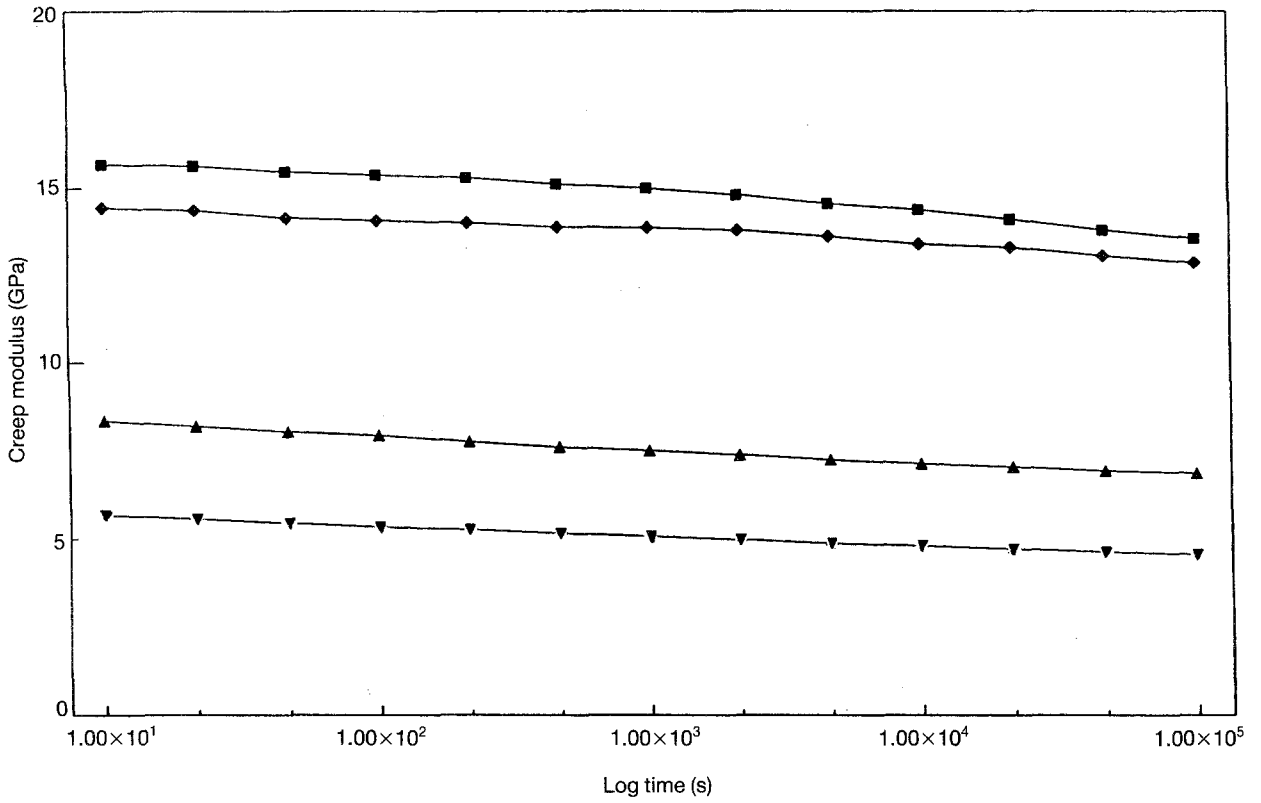

Figure 7 Tensile creep modulus functions for 50% wt/wt (■,▲) LF GL/PA and (◆, ▼) SF GL/PA, multilive feed processed, at (■, ◆) 23°C and (▲, ▼) 120°C.

TABLE IX Mean fibre lengths for the long and short glass fibre nylon multilive feed compounds, compared to the critical fibre lengths for the compounds as determined from Table IV at matrix modulus values of 2.8 and 0.5 GPa, corresponding to the low strain modulus values at 23 and 120 °C, respectively. The final column list the percentage of fibres in each compound that exceed the critical fibre lengths at the two temperatures, as determined from Fig. 6

Material	Mean fibre length $\langle l \rangle$ (μm)	l_c(μm)		Fibres with lengths $> l_c$ (%)
		23°C	120°C	
Long-fibre GL/PA	580	167	396	98% (23 °C) 75% (120 °C)
Short-fibre GL/PA	210	98	233	85% (23 °C) 32% (120 °C)

TABLE X 100 s creep modulus data at 23 and 120 °C for the long and short glass fibre nylon multilive feed compounds, compared to predicted modulus values as determined from Figs 4 and 5 at matrix modulus values of 2.8 and 0.5 GPa, corresponding to the low strain modulus values at 23 and 120 °C, respectively. The long-fibre compound assumes a mean fibre length of 0.6 mm and the short-fibre compound assumes a mean fibre length of 0.2 mm. The final row list the percentage reduction in the modulus between the short and long-fibre compound at each temperature

Material	$E(0.2\%)$ (GPa)			
	Experiment, $t = 100$ s		Prediction, $t = 100$ s	
	$T = 23$ °C	$T = 120$ °C	$T = 23$ °C	$T = 120$ °C
Long-fibre GL/PA	15.38	7.94	22.70	18.94
Short-fibre GL/PA	14.09	5.37	20.59	14.37
Difference between long and short GL/PA compounds (%)	91.2	67.6	90.7	75.8

temperature of 120 °C, the nylon matrix modulus drops to approximately 0.5 GPa. The critical fibre lengths for the two materials correspondingly increase at the higher temperature. However, due to the longer fibre lengths achieved in the long-fibre compound, a much greater percentage of the fibres exceed the critical fibre length (75% of fibres $> l_c$) compared to the percentage for the short-fibre compound (32% of fibres $> l_c$). This explains why the long-fibre compound has a much improved stiffness at 120 °C compared to the short-fibre compound. Referring to Figs 4 and 5 provides another source of explanation for the effect noted experimentally. Fig. 4 shows that for a glass-fibre compound with 50% wt/wt glass fibre (diameter 17 μm) and a mean fibre length of approximately 0.6 mm should produce a composite with a modulus of 22.7 GPa at 23 °C and 18.94 GPa at 120 °C. The equivalent data for the short-fibre compound with the same weight fraction of fibres (with 10 μm diameter) should produce a composite with a modulus of 20.59 GPa at 23 °C and 14.37 GPa at 120 °C. In Table X the actual modulus data taken from Fig. 7 are compared to these predictions and the relative difference between the two compounds has also been calculated.

The predictions are an overestimate of the measured performance by a factor of approximately 0.67 at 23 °C and 0.4 at 120 °C and are due to fibre orientation and fibre length distribution effects in the real compounds. However, the model given by Equation 14 successfully predicts the relative fall in modulus between the two types of compound at the elevated temperature as can be seen from Table X.

This effect has also been observed at intermediate temperatures and for moisture-conditioned specimens, where the nylon matrix loses stiffness through plasticization and will be dealt with in a future publication.

5. Conclusions

This paper has reviewed the simple theory for fibre reinforcement and its application to discontinuous fibre composites. The available scientific evidence based on micromechanical experiments of single-fibre composites using Raman spectroscopy and fibre fragmentation tests tends to support the findings of this theory. The scientific literature suggests that there is a strong correlation between mechanical properties such as stiffness, strength and toughness with an increased fibre aspect ratio.

It is worth stressing some of the key points to emerge from this study.

1. The Cox model represents the behaviour for uniaxially oriented discontinuous fibre composite materials in the limit of low strain ($\varepsilon_c < 0.50\%$), which is often the practical limit of strain applied to these types of materials in service.
2. The prediction of critical fibre length, via Equation 8, leading to the observation that the critical fibre length depends directly upon fibre and matrix tensile moduli, fibre volume fraction, and fibre diameter, providing the bonding is good and no interfacial breakdown mechanisms have occurred.
3. Critical fibre lengths produced from single-fibre tests are often overestimating the value for l_c that exist in more practical composites with higher volume fractions.
4. For effective uniaxial discontinuous fibre composite performance (defined as 90% the stiffness achieved by an equivalent continuous fibre composite), the mean fibre length should be greater or equal to four times the predicted critical fibre length.
5. For a given weight fraction of fibres, mean fibre length and matrix modulus, a stiffer and tougher composite will be made from using a smaller fibre diameter, to an observed practical limit of about 7 μm.
6. The use of longer fibres at a particular fibre diameter will necessarily make a stiffer and tougher composite.

It is worth stressing that the predictions for the critical aspect ratio are for the case of uniaxial orientation, which approximate to the skin regions in the direction of the melt flow front in conventional injection mouldings, or to composites produced by multiple live feed technology. For fibres oriented at an angle to the applied stress field, or in the case of poor bonding, the reinforcing efficiency of the fibres will fall. Consequently, these predictions represent the lower bound for the critical fibre length in these materials.

Real discontinuous fibre composites are extremely complicated in terms of their microstructure, so the simple predictions for the micromechanics of such materials based upon the Cox model have their limits.

Nonetheless, the detail described in Sections 2 and 3 seems to be in accord with the available experimental evidence as outlined in Sections 3.2 and 4. A simple model of a unidirectional discontinuous fibre composite can be used as the basis for a more complicated model, representing more realistic microstructures in injection-moulded parts, as described by Davies *et al.* [31]. This model assumes that complicated microstructures with a range of fibre orientations can be modelled as a series of non-interacting layers based on the mechanics of uniaxial discontinuous fibre composites, with each layer given an associated angle to represent the orientation distribution effect and a fibre length distribution. This approach has successfully modelled a wide range of injection-moulded structures, including real component geometries. [31, 32].

Given the predictions contained in Sections 2 and 3 and the experimental observations in the scientific literature, the present study indicates that the attainment of fibre lengths which exceed the critical aspect ratio for the compound over the full range of service conditions, such as time and temperature, is essential for a high-performing discontinuous fibre-reinforced compound.

Acknowledgements

The authors wish to acknowledge useful discussions and contributions from R. S. Bailey, G. von Bradsky, C. Galiotis, D. R. Moore and I. D. Newton.

References

1. *Eur. Plastics News* (March) (1993) 21.
2. H. L. COX, *Br. J. Appl. Phys.* **3** (1952) 72.
3. G. S. HOLLISTER and C. THOMAS, "Fibre Reinforced Materials" (Elsevier, 1966).
4. T. S. CHOW, *J. Mater. Sci.* **15** (1980) 1873.
5. E. I. M. ASLOUN, M. NARDIN and J. SCHULZ, *ibid.* **24** (1989) 1835.
6. C. GALIOTIS, *Compos. Sci. Technol.* **42** (1991) 125.
7. C. GALIOTIS, R. J. YOUNG, P. H. J. YEUNG and D. N. BATCHELDER *J. Mater. Sci.* **19** (1984) 3640.
8. L. MONETTE, M. P. ANDERSON, S. LING and G. S. GRIST, *ibid.* **27** (1992) 4393.
9. B. W. ROSEN, *AIAA J.* **2** (1964) 1985.
10. Y. TERMONIA, *J. Mater. Sci.* **22** (1987) 504.
11. M. R. PIGGOTT, *Polym. Compos.* **8** (1987) 291.
12. *Idem, Compos. Sci. Technol.* **42** (1991) 57.
13. J. C. FIGUEROA, T. E. CARNEY, L. S. SCHADLER and C. LAIRD, *ibid.***42** (1991) 77.
14. M. NARKIS, E. J. H. CHEN and R. B. PIPES, *Polym. Compos.* **9** (1988) 245.
15. N. MELANITIS and C. GALIOTIS, *Proc. R. Soc. Lond. A* **440** (1993) 379.
16. R. J. YOUNG, in "Polymer surfaces and interfaces II", edited by W. J. Feast, H. S. Munro and R. W. Richards (Wiley, 1993) Ch. 6.
17. R. J. DAY and R. J. YOUNG, *J. Micros.* **169** (1993) 151.
18. C. GALIOTIS, R. J. YOUNG, P. H. J. YEUNG and D. N. BATCHELDER, *J. Mater. Sci.* **19** (1984) 3640.
19. I. M. ROBINSON, P. H. J. YEUNG, R. J. YOUNG and C. GALIOTIS, *ibid.* **21** (1986) 3642.
20. I. M. ROBINSON, R. J. YOUNG, C. GALIOTIS and D. N. BATCHELDER, *ibid.* **22** (1987) 3642.
21. I. M. ROBINSON, C. GALIOTIS, D. N. BATCHELDER and R. J. YOUNG, *ibid.* **26** (1991) 2293.
22. H. JAKANKHANI and C. GALIOTIS, *J. Compos. Mater.* **25** (1991) 609.
23. M. C. ANDREWS and R. J. YOUNG, *J. Raman Spec.*
24. M. C. ANDREWS, R. J. DAY, X. HU and R. J. YOUNG, *J. Mater. Sci. Lett* **11** (1992) 1344.
25. N. MELANITIS, C. GALIOTIS, P. L. TETLOW and C. K. L. DAVIES, *J. Compos. Mater.* **26** (1992) 574.
26. N. MELANITIS, C. GALIOTIS, P. L. TETLOW and C. K. L. DAVIES *J. Mater. Sci.* **28** (1993) 1648.
27. W. D. BASCOM and R. M. JENSEN, *J. Adhesion* **19** (1986) 219.
28. A. T. DIBENEDETTO, *Compos. Sci. Technol.* **42** (1991) 103.
29. N. LAWS and R. McLAUGHLIN, *J. Mech. Phys. Solids* **27** (1979) 1.
30. C. R. GORE, G. CUFF and D. A. CIANELLI, *Mater. Eng.* **103** (1986) 47.
31. M. DAVIES, R. S. BAILEY and D. R. MOORE, *Composites* **20** (1989) 453.
32. D. R. MOORE, I. M. ROBINSON and B. SLATER, in "FRC 90" (Institute of Mechanical Engineers, London, 1990) p. 203.
33. R. S. BAILEY and H. KRAFT, *Int. Polym. Proc.* **2** (1987) 94.
34. R. S. BAILEY, D. R. MOORE, I. M. ROBINSON and P. M. RUTTER, *Sci. Eng. Compos. Mater.* **2** (1993) 171.
35. M. J. CARLING and J. G. WILLIAMS, *Polym. Compos.* **11** (1990) 307.
36. F. RAMSTEINER and R. THEYSOHN, *Compos. Sci. Technol.* **24** (1985) 231.
37. *Idem, Composites* **10** (1979) 111.
38. F. RAMSTEINER, *ibid.* **12** (1981) 65.
39. N. SATO, T. KURAUCHI, S. SATO and O. KAMIGAITO, *J. Compos. Mater.* **22** (1988) 850.
40. M. AKAY and D. BARKLEY, *J. Mater. Sci.* **26** (1991) 2731.
41. N. SATO, T. KURAUCHI, S. SATO and O. KAMIGAITO, *J. Mater. Sci.* **26** (1991) 3891.
42. S. TURNER, *Br. Plast.* (April) (1972) p. 7.

Received 7 April
and accepted 11 June 1993